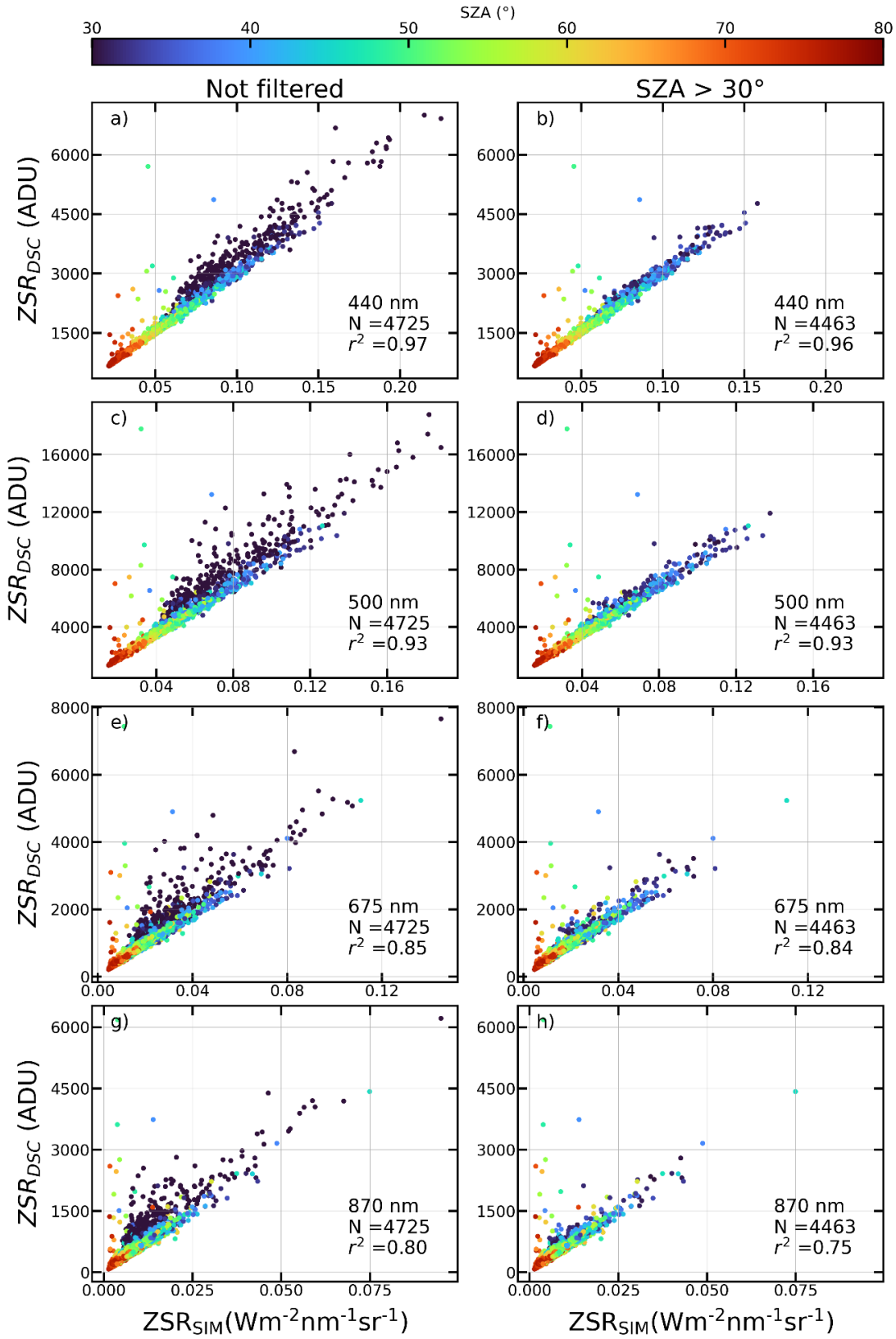
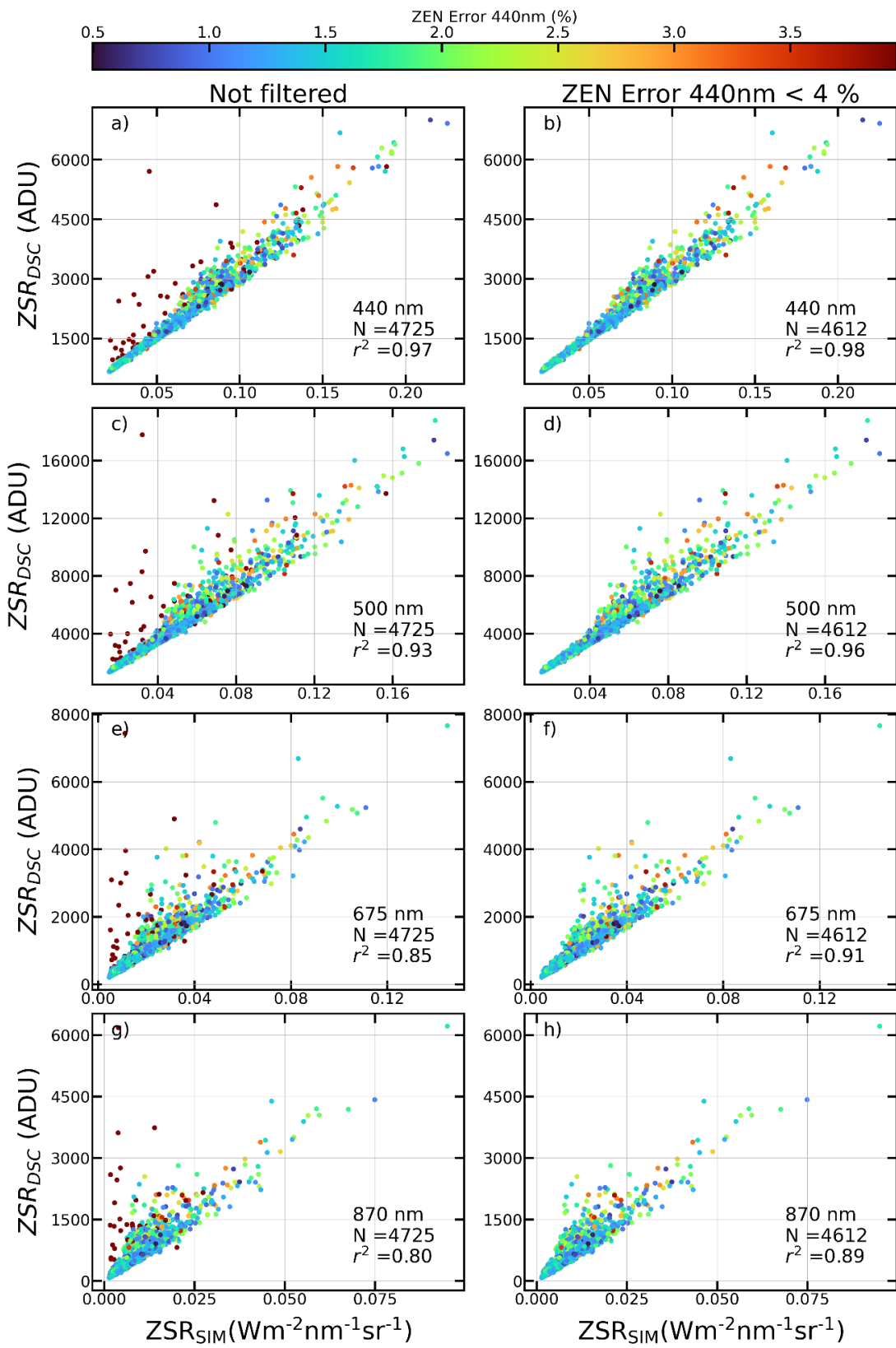


**Figure S1.** Aerosol size distribution for each aerosol type considered by the GRASP-ZEN inversion approach.



**Figure S2.** Scatter plot of the measured zenith sky radiances corrected from dark signal ( $ZSR_{DSC}$ ), in analog-to-digital units (ADU), against the zenith sky radiances simulated by GRASP ( $ZSR_{SIM}$ ), both at 440 nm (upper panels), 500 nm (second row panels), 675 nm (third row panels) and 870 nm (bottom panels). Left and right panels show these data respectively before and after applying the SZA quality control filtering. Determination coefficient ( $r^2$ ) and number of data pairs (N) are also shown. Points colours represent the corresponding SZA.



**Figure S3.** Scatter plot of the measured zenith sky radiances corrected from dark signal (ZSR<sub>DSC</sub>), in analog-to-digital units (ADU), against the zenith sky radiances simulated by GRASP (ZSR<sub>SIM</sub>), both at 440 nm (upper panels), 500 nm (second row panels), 675 nm (third row panels) and 870 nm (bottom panels). Left and right panels show these data respectively before and after applying the ZEN error quality control filtering. Determination coefficient ( $r^2$ ) and number of data pairs (N) are also shown. Points colours represent the corresponding ZEN error.

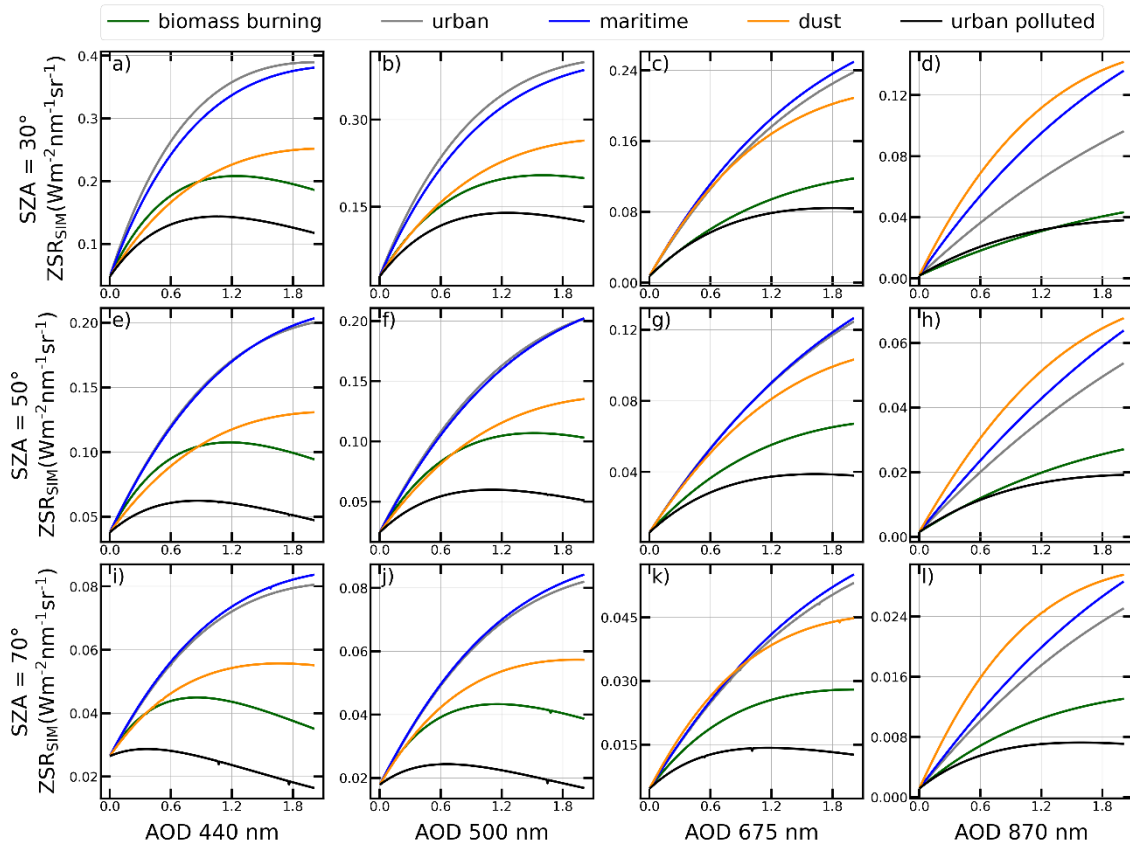


**Figure S4.** Zenith sky radiances (ZSR) modelled with GRASP for different aerosol concentrations at the four wavelength and for SZA = 30 (a-d), 50 (e-h) and 70° (i-l) for the different aerosol types from the ‘models’ method from GRASP.

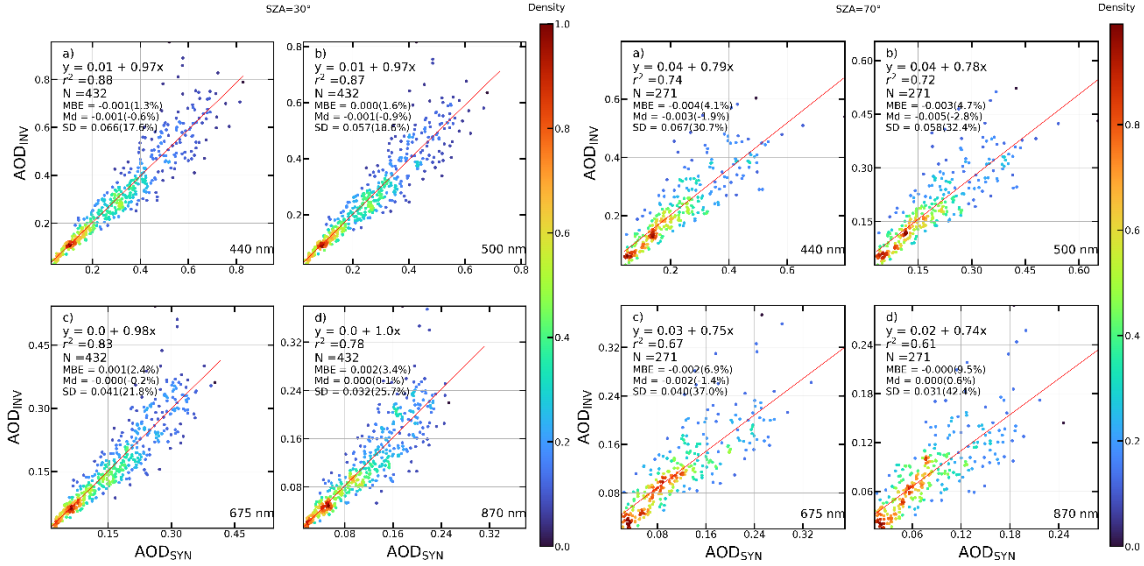


**Figure S5.** Left panel. Density scatter plot of the AOD retrieved by GRASP after the inversion of synthetic ZSR (AOD<sub>INV</sub>) against the initial AOD (AOD<sub>SYN</sub>) obtained for synthetic scenarios created from the combination of five aerosol types for SZA=30° at a) 440nm, b) 500nm, c) 675 nm and d) 870 nm. Linear fit (red line) with its equation, determination coefficient ( $r^2$ ) and number of data points (N) are shown. Mean bias error (MB), median (Md) and standard deviation (SD) of the absolute and  $\Delta$  (between brackets) differences between the inverted and synthetic AOD are also included. Right panel. Same plot for SZA=70°.

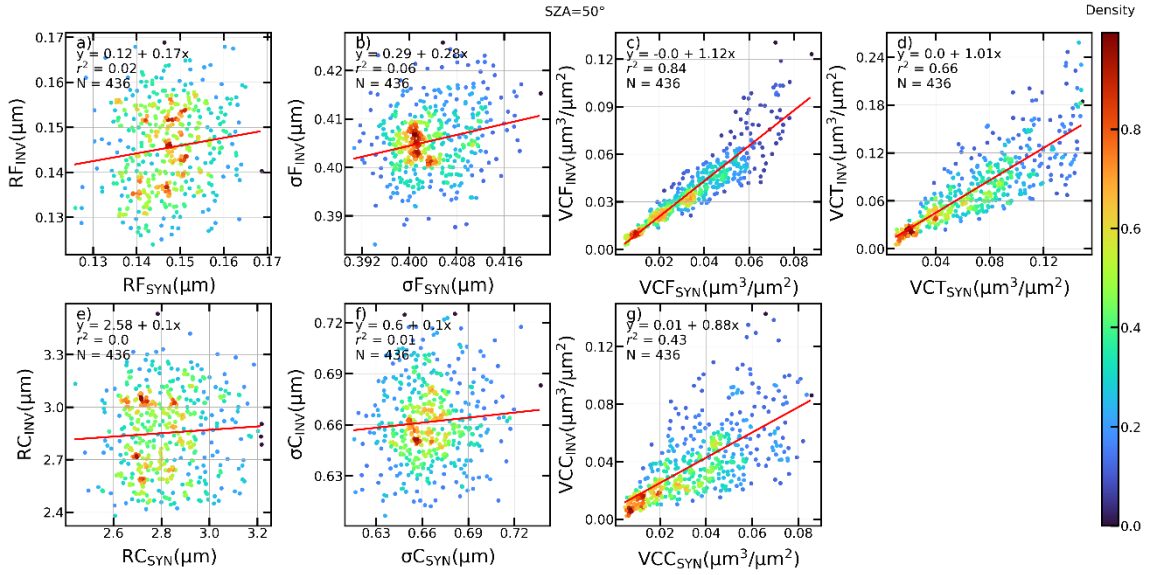


**Figure S6.** Density scatter plot of the aerosol size distribution properties retrieved by GRASP after the inversion of synthetic ZSR (INV) against the ones initially obtained (SYN) for synthetic scenarios created from the combination of five aerosol types for SZA=50°. Linear fit (red line) with its equation, determination coefficient ( $r^2$ ) and number of data points (N) are shown. These size distribution properties are volume median radius of fine (RF) and coarse (RC) modes, standard deviation of log-normal distribution for fine ( $\sigma$ F) and coarse ( $\sigma$ C) modes, and aerosol volume concentration for fine (VCF) and coarse (VCC) modes and the total (VCT).

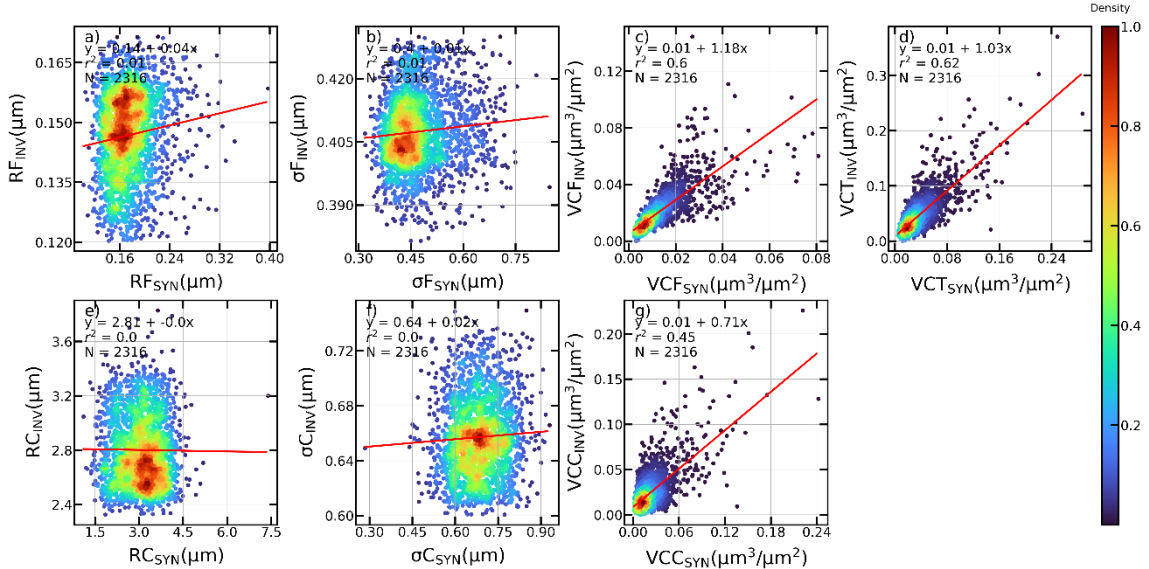


**Figure S7.** Density scatter plot of the aerosol size distribution properties retrieved by GRASP after the inversion of synthetic ZSR (INV) against the ones initially obtained (SYN) for synthetic scenarios obtained from AERONET retrievals. Linear fit (red line) with its equation, determination coefficient ( $r^2$ ) and number of data points (N) are shown. These size distribution properties are volume median radius of fine (RF) and coarse (RC) modes, standard deviation of log-normal distribution for fine ( $\sigma$ F) and coarse ( $\sigma$ C) modes, and aerosol volume concentration for fine (VCF) and coarse (VCC) modes and the total (VCT).